OXFORD GENETICS

GENETICS, 2025, iyaf107
https://doi.org/10.1093/genetics/iyaf107
Advance Access Publication Date: 10 June 2025
Investigation

Analysis of combinatorial cohesin subunit gene deletions in budding yeast

Grace Duke,[1] Robert V. Skibbens [2,*]

[1]Department of Bioengineering, Lehigh University, 111 Research Drive, Bethlehem, PA 18015, USA
[2]Department of Biological Sciences, Lehigh University, 111 Research Drive, Bethlehem, PA 18015, USA

*Corresponding author: Email: rvs3@lehigh.edu

Throughout the cell cycle, DNA molecules convert between hierarchical intramolecular (cis) and intermolecular (trans) associations. Cohesin ATPase complexes produce both types of DNA associations which collectively are required for sister chromatid segregation, chromatin condensation, genomic architecture, gene transcription, and DNA repair. The mechanisms that regulate cohesin cis- and trans-activities, however, remain controversial. A popular model is that a regulatory complex (Pds5, Irr1/Scc3, and Rad61) sits atop a core ring-like complex (Mcd1/Scc1, Smc1, and Smc3), the latter of which exhibits the inherent ATPase activities responsible for producing cis- and trans-DNA conformations. Additional proteins transiently interact with cohesins to promote cohesin deposition onto DNA (Scc2 and Scc4) or stabilize cohesin-DNA binding (Eco1/Ctf7). Of these 9 components, only *RAD61* is nonessential. Recent findings, however, identified pairs of suppressor mutations that support the viability of cells individually deleted for either *PDS5* or *ECO1/CTF7* (herein *ECO1*). Intriguingly, *CLN2* deletion is common in both suppressor pairs, suggesting that combined suppressor mutations may support the viability of cells co-deleted for both *ECO1* and *PDS5*. These results further suggest that the addition of other suppressor mutations (such as *ELG1* and *RAD61*) may support the viability of cells deleted of all auxiliary subunits—including *IRR1/SCC3* (herein *SCC3*). Here, we test these predictions and report on novel gene deletion combinations required for cell cycle progression and cell viability.

Keywords: cohesinopathies; Roberts syndrome (RBS); Cornelia de Lange syndrome (CdLS); *ECO1/CTF7(EFO1/ESCO1,EFO2/ESCO2)*; cohesin; *SMC3*; *SMC1*; *SCC31/IRR1(STAG1,STAG2,STAG3)*; *PDS5*; *RAD61(WAPL)*; *MCD1/SCC1(RAD21)*; *CLN2(CCNA-CCNE)*; *ELG1/RTT110(ATAD5)*

Introduction

Cohesins are DNA-binding ATPases that perform 2 highly conserved activities: cis-based looping (termed extrusion) and trans-based tethering (termed cohesion). Collectively, these processes produce the various DNA conformations required for gene transcription, chromosome segregation, chromatin condensation, and DNA repair. For instance, each chromosome within the G1 cell cycle phase coalesces into a distinct territory that can further partition into topologically associated domains (TADs), compartments, and other various states of organization. Intramolecular loops of DNA, extruded by cis-based cohesin activities, help delineate regions of transcription in which hundreds of genes might be coordinately induced or repressed (Fritz *et al.* 2019; Skibbens 2019; Karpinska and Oudelaar 2023; Zhang and Blobel 2023). In contrast, sister chromatids become tethered together during S phase in a process coupled to DNA replication (Skibbens *et al.* 1999). This tethering, produced by trans-based cohesin activities, ensures high fidelity chromosome segregation during mitosis (Nishiyama 2019; Zuilkoski and Skibbens 2022; Horsfield 2023). Cis- and trans-based cohesin activities, however, are not separated across the cell cycle. Chromosome condensation during mitosis is facilitated through cis-based cohesin activities (Guacci *et al.* 1997; Skibbens 2019; Konecna *et al.* 2023; McAinsh and Kops 2023) while TADs from different chromosomes can become tethered together during G1 through trans-based cohesin activities (Luppino *et al.* 2020; Liyakat Ali *et al.* 2021; Chang and Noordermeer 2024).

While little is known regarding cohesin regulation across the cell cycle, much is known of cohesin structure (Fig. 1). Cohesin core subunits (Mcd1, Smc1, and Smc3) form a ring-like structure which harbors cohesin ATPase activity (Skibbens 2019; Horsfield 2023; Golov and Gavrilov 2024). In turn, Mcd1 recruits auxiliary subunits (Pds5, Rad61, and Scc3/Irr1—herein Scc3) to form a cohesin holocomplex (Kueng *et al.* 2006; Rowland *et al.* 2009; Sutani *et al.* 2009; Kulemzina *et al.* 2012). Additional components regulate the inherent ATP activity of cohesins. For instance, cohesin deposition onto DNA requires the loader heterodimer Scc2 and Scc4 complex (Ciosk *et al.* 2000; Rollins *et al.* 2004; Tonkin *et al.* 2004; Watrin *et al.* 2006) while Rad61 promotes cohesin dissociation from DNA. During DNA replication, cohesin dissociation is blocked by Eco1/Ctf7 (herein Eco1)—an acetyltransferase that modifies Smc3 to render cohesin insensitive to Rad61 (Skibbens *et al.* 1999; Tóth *et al.* 1999; Ivanov *et al.* 2002; Bellows *et al.* 2003; Hou and Zou 2005; Vega *et al.* 2005; Rolef Ben-Shahar *et al.* 2008; Unal *et al.* 2008; Zhang *et al.* 2008). Eco1 family members (EFO1/ESCO1 and EFO2/ESCO2 in humans) and Rad61 (WAPL in humans) also regulate loop extrusion during G1 and chromosome condensation during M phase (Skibbens *et al.* 1999; Bellows *et al.* 2003; Hou and Zou 2005; Vega *et al.* 2005; Gard *et al.* 2009; Guacci and Koshland 2012;

Received on 04 April 2025; accepted on 27 May 2025
© The Author(s) 2025. Published by Oxford University Press on behalf of The Genetics Society of America. All rights reserved. For commercial re-use, please contact reprints@oup.com for reprints and translation rights for reprints. All other permissions can be obtained through our RightsLink service via the Permissions link on the article page on our site—for further information please contact journals.permissions@oup.com.

Downloaded from https://academic.oup.com/genetics/advance-article/doi/10.1093/genetics/iyaf107/8156691 by guest on 23 June 2025

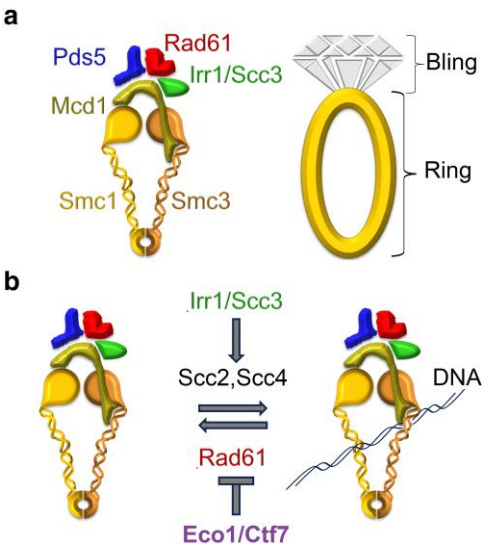

Fig. 1. Cohesin complex and regulators. a) Schematic of a cohesin holocomplex—following the prior analogy of cohesin as an engagement ring (Remeseiro and Losada 2013). Mcd1, a key component of the core ring complex (Mcd1-Smc1-Smc3), recruits several auxiliary subunits (Pds5-Rad61-Irr1/Scc3). The auxiliary complex, shown to the right as the diamond "bling" atop an engagement ring, is thought to regulate the ATPase activities of core ring subunits Smc1 and Smc3. b) Cohesin deposition onto DNA (right image) requires the loader complex Scc2 and Scc4. Loading complex recruitment is facilitated by Scc3/Irr1, a component of auxiliary complex. Once loaded, cohesin can dissociate from DNA, a process promoted by the auxiliary component Rad61. Eco1/Ctf7 acetylation of Smc3 blocks Rad61 activity. See text for details.

Lopez-Serra *et al.* 2013; Tedeschi *et al.* 2013; Tong and Skibbens 2015; Dauban *et al.* 2020; Wutz *et al.* 2020; Barton *et al.* 2022).

Identification of bypass suppressors provides important insights into the function of individual cohesin subunits. In human cell lines, depletion of WAPL (human homolog of yeast Rad61) suppresses the premature sister chromatid cohesion defect that otherwise arises in response to depletion of ESCO2 (human homolog of Eco1) (Bellows *et al.* 2003; Hou and Zou 2005; Vega *et al.* 2005; Gandhi *et al.* 2006). In yeast, deletion of *RAD61* rescues both the cohesion defects and inviability of cells deleted of *ECO1* (Rowland *et al.* 2009; Sutani *et al.* 2009), although double-mutated *eco1Δ rad61Δ* cells (*Δ* herein refers to gene deletion) exhibit temperature-sensitive (ts) lethality (Maradeo and Skibbens 2010; Buskirk and Skibbens 2022). This ts growth defect is rescued by further deletion of *CLN2* (Buskirk and Skibbens 2022). While the mechanism remains to be determined, G1 cyclin-dependent kinase (CDK) activity reduces Mcd1 levels (Psakhye and Branzei 2021; Choudhary *et al.* 2022; Singh and Skibbens 2024) such that elevated expression of *MCD1* is sufficient to rescues *eco1Δ rad61Δ* cell ts lethality (Singh and Skibbens 2024). Cells deleted of *PDS5* also contain low levels of Mcd1, but deletions of both *CLN2* and *ELG1* support *pds5Δ* cell viability (Choudhary *et al.* 2022). Elg1 is a component of the RFC (replication factor C complex) that unloads the sliding clamp PCNA from the DNA replication fork (Shiomi and Nishitani 2017; Arbel *et al.* 2021). Cells deleted of *ELG1* retain elevated levels of chromatin-bound PCNA, which in turn recruits both Eco1 and Scc2 and thereby couples cohesion establishment to chromosome replication (Skibbens *et al.* 1999; Kenna and Skibbens 2003; Moldovan *et al* 2006; Higashi *et al.* 2012; Zhang *et al.* 2017; Bender *et al.* 2020; Zuilkoski and Skibbens 2020; Yoshimura *et al.* 2021; van Schie *et al.* 2022; Psakhye *et al.* 2023).

In this current study, we test the extent to which novel combinations of suppressor mutations support the viability of cells co-deleted for *ECO1* and *PDS5*, as well the auxiliary-encoding gene *SCC3*, with the goal of identifying inherent cohesin activities devoid of auxiliary components.

Materials and methods

Yeast strains and media

Generation of 6 gene deletion (6del) heterozygous diploid strains (YBS3992-3995) proceeded following standard yeast genetics and molecular biological techniques. Briefly, *pds5-1* cells (VG986-5B) (Hartman *et al.* 2000) were backcrossed 5 times into standard W303 wild-type (WT) cells to produce YMM526. *pds5-1* (YMM526) was then crossed to *elg1Δ::kanMX6* cells (YMM288), the latter produced via transformation of gene-replacement PCR product as previously described (Longtine *et al.* 1998; Maradeo and Skibbens 2009). Resulting *ELG1/elg1Δ::kanMX6 PDS5/pds5-1* diploids were sporulated with subsequent dissections used to identify *elg1Δ::kanMX6 pds5-1* haploid strains (YMM621-YMM623). Two independent isolates of *elg1Δ::kanMX6 pds5-1* cells (YMM621 and YMM623) were each mated to YBS3544 (*eco1Δ::HIS3 rad61Δ::URA3 cln2Δ::kanMX6*) (Buskirk and Skibbens 2022) to produce 4 deletion (4del) heterozygous diploid strains *ELG1/elg1Δ::kanMX6 PDS5/pds5-1 ECO1/eco1Δ::HIS3 RAD61/rad61Δ::URA3 CLN2/cln2Δ::kanMX6* (independent isolates YBS3740 and YBS3742). YBS3740 and YBS3742 were then each transformed with gene-replacement PCR products engineered to replace *PDS5* with *TRP1* (oligos oRVS3279 and oRVS3238 and template pBS1039) (Longtine *et al.* 1998). Proper integration (*pds5Δ::TRP1*) of TRP+ transformants was confirmed by PCR (oRVS3276, oRVS8, oRVS3276, and oRVS3278). The resulting 5del diploid strains YBS3983 (derived from YBS3740) and YBS3986 (derived from YBS3742) were then each transformed with gene-replacement PCR products engineered to replace *SCC3/IRR1* with *cloNAT* (oligos oRVS327 and oRVS3295 and template pAG25). Proper integration (*SCC3Δ::cloNAT*) of Nourseothricin+ transformants was confirmed by PCR (oRVS3273 and oRVS3277). Four independent 6del diploids (YBS3992 and YBS3993 derived from YBS3983; YBS3994 and 3995 derived from YBS3986) were used for further analyses.

Final validation of 6del strains were performed using the following primer pairs: *TRP1* replacement of *PDS5* was confirmed using primers 8 and 3276; *kanMX6* replacement of *ELG1* was confirmed using primers 23 and 238; *HIS3* replacement of *ECO1* was confirmed using primers 9 and 254; *cloNAT* replacement of *SCC3* was confirmed using primers 179 and 3273; *URA3* replacement of *RAD61* was confirmed using primers 113 and 258; and *kanMX6* replacement of *CLN2* was confirmed using primers 23 and 3197. The following PCR reactions confirmed retention of the WT copy of the cohesin genes in our 6del strains: *PDS5* was confirmed using primers 3239 and 3278; *ELG1* was confirmed using primers 121 and 122; *ECO1* was confirmed using primers 3333 and 255; *SCC3/IRR1* was confirmed using primers 3339 and 3340; *RAD61* was confirmed using primers 258 and 3389; and *CLN2* was confirmed using primers 3197 and 3388. Additional primers, and all primer sequences used throughout this study, are listed in Supplementary Table 1. Yeast strains listed in the study are contained in Table 1.

Growth and ploidy analyses

Log phase cultures of WT (YBS255) and 2 independent 6del isolates (YBS3992 and YBS3995) were serially diluted onto rich media

Downloaded from https://academic.oup.com/genetics/advance-article/doi/10.1093/genetics/iyaf107/8159691 by guest on 23 June 2025

Table 1. Strains used in this study.

Strains	Genotypes	References
YPH499	*MAT***a** *ura3-52 lys2-801_amber ade2-101_ochre trp1-Δ63 his3-Δ200 leu2-Δ1*	Sikorski and Hieter 1989
YBS255	*MAT***a** *ura3-52 lys2-801 ade2-101 trp1-Δ63 his3-Δ200 leu2-Δ1 ctf7Δ1::HIS3 CTF7:LEU2*	Skibbens *et al.* 1999
YBS3544	*MAT***a** *ade2-101 his3Δ200 leu2Δ1 lys2-801 trp1Δ63 ura3-52 cft7::HIS3 rad61::URA3 cln2::KAN*	Buskirk and Skibbens 2022
YBS3992	*MAT***a/α** *ECO1/eco1Δ RAD61/rad61Δ PDS5/pds5Δ ELG1/elg1Δ CLN2/cln2Δ*	Current study
YBS3995	*MAT***a/α** *ECO1/eco1Δ RAD61/rad61Δ PDS5/pds5Δ ELG1/elg1Δ CLN2/cln2Δ* (independent isolate of 3992)	Current study
YBS4141	*MAT***a** *ura3-52 lys2-801 ade2-101 trp1-Δ63 his3-Δ200 leu2-Δ1 eco1Δ rad61Δ pds5Δ elg1Δ cln2Δ*	Current study
YBS4176	*MAT***a** *ura3-52 lys2-801 ade2-101 trp1-Δ63 his3-Δ200 leu2-Δ1 eco1Δ pds5Δ elg1Δ cln2Δ*	Current study
YBS4268	*MAT***α** *ura3-52 lys2-801 ade2-101 trp1-Δ63 his3-Δ200 leu2-Δ1 eco1Δ pds5Δ elg1Δ cln2Δ*	Current study
YBS4245*	*eco1Δ rad61Δ elg1Δ* *Independent isolates YBS4248, YBS4262, YBS270, YBS4291, YBS4297, and YBS4304	Current study
YMM288	*MAT***a** *ade2-1 his3-11,15 leu2-3,112 trp1-1 ura3-1 can1-100 elg1::kanMX6 (isolate 1A)*	Current study
YMM526	*MAT***alpha** *ade2-1 his3-11,15 leu2-3,112 trp1-1 ura3-1 can1-100 pds5-1 (isolate 4B)*	Current study
YMM621	*MAT***a** *ade2-1 his3-11,15 leu2-3,112 trp1-1 ura3-1 can1-100 pds5-1 elg1::kanMX6 (isolate 1D)*	Current study
YMM623	*MAT***a** *ade2-1 his3-11,15 leu2-3,112 trp1-1 ura3-1 can1-100 pds5-1 elg1::kanMX6 (isolate 3C)*	Current study
YMM828	*MAT***alpha** *eco1^{ctf7}::HIS3 rad61::URA3 ade2-101 his3Δ200 leu2Δ1 lys2-801 trp1Δ63 ura3-52*	Maradeo and Skibbens 2010
VG986-5B	*MATa trp1 ura3 bar1 gal1*	Hartman *et al.* 2000

plates and then incubated at the indicated temperatures (23, 30, and 37°C).

Log phase cultures of WT (YBS255) and 2 independent 6del isolates (YBS3992 and YBS3995) were fixed and prepared for flow cytometry analysis (BD FACScan) as previously described (Gerring *et al.* 1990; Maradeo and Skibbens 2009). DNA contents (1C and 2C) were based on log phase growth profiles obtained for each strain.

Western blot analyses

Cell extracts and Western blot analyses were performed as previously described (Tong and Skibbens 2014; Mfarej and Skibbens 2020). DNA damage was induced by exposing the liquid cell culture to methyl methanesulfonate (MMS) (Sigma) at a final concentration of 0.1% for the time indicated. Rad53 detection was performed using anti-Rad53 (Santa Cruz, yC-19) followed by donkey-anti-goat HRP (Abcam, ab97110).

Condensation/cohesion assays

Condensation/cohesion assays were performed as previously described (Shen and Skibbens 2017, 2020). Briefly, log phase cultures were either shifted to rich medium containing nocodazole (NZ) and maintained at 37°C for 3 h or presynchronized in either alpha factor (G1 arrest) or hydroxyurea (early S phase arrest) at 30°C before washing and shifting to rich medium containing NZ as described above. Preanaphase synchronized cells were fixed (3.7% formaldehyde) and washed before resuspending in spheroplast buffer (1 M sorbitol, 20 mM KPO4, pH7.4, β-mercaptoethanol, and Zymolyase T100). Spheroplasted cells were pelleted, resuspended in spheroplast buffer supplemented with 0.5% Triton X-100, and then affixed to poly-L-lysine coated slides. Cell lysis was performed by the addition of 0.5% SDS before immersing in 3:1 methanol:acetic acid. The DNA masses were incubated in RNase (100 μg/mL) in 2× SSC buffer (0.3 M NaCl, 30 mM sodium citrate, pH7.0), and washed in 2× SSC prior to dehydration through a series of −20°C ethanol washes. Denaturation (70% formamide, 2× SSC) at 72°C for 2 min was immediately followed by a series of −20°C dehydration steps and allowed to air dry. DNA was detected by DAPI (0.05 μg/mL) staining and assayed under a microscope [Nikon E800 equipped with CD camera (CoolSnap FX, Photometrics) and software package (IPLab, Scanalytics, Inc.)].

Results

Characterization of 6-gene deletion diploid strains

To test for genetic combinations that support the viability of cells deleted for essential cohesin genes, diploid strains heterozygous null for *PDS5*, *ECO1*, *SCC3*, *CLN2*, *ELG1*, and *RAD61* were generated via a multistep process (see Materials and methods). The heterozygous composition of the resulting 6-gene deletion (herein 6del) strains was confirmed by PCR (Supplementary Fig. 1). *PDS5*, *ECO1*, and *SCC3* are essential genes that ensure euploidy during cell division (Michaelis *et al.* 1997; Kurlandzka *et al.* 1999; Skibbens *et al.* 1999; Tóth *et al.* 1999; Hartman *et al.* 2000; Panizza *et al.* 2000). Despite the heterozygous deletion of all 3 essential genes, 6del isolates produced DNA histograms consistent with a euploid diploid genome (Fig. 2b; Supplementary Fig. 2). Growth defects commonly arise across a wide range of model systems in response to heterozygous deletions (Birchler and Veitia 2021; Chunduri *et al.* 2022). To test for growth defects in our 6del strains, log phase cultures of WT (YBS255) and 2 6del isolates (YBS3992 and YBS3995, herein 3992 and 3995) were serially diluted onto rich media plates and then incubated at 23, 30, and 37°C. Both 6del strains exhibited growth nearly identical to that of WT cells across all temperatures tested (Fig. 2c). Thus, the combinatorial heterozygous deletion of 3 essential genes (*ECO1*, *SCC3*, and *PDS5*) did not produce overt growth

Downloaded from https://academic.oup.com/genetics/advance-article/doi/10.1093/genetics/iyaf107/8159691 by guest on 23 June 2025

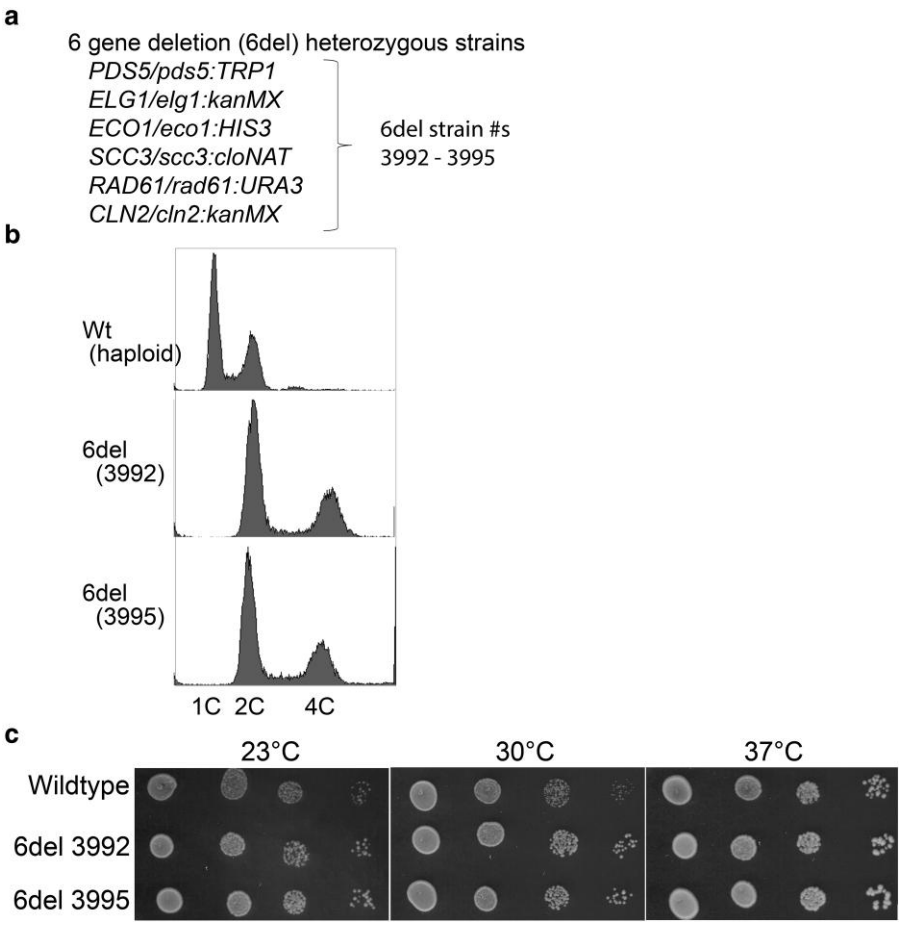

Fig. 2. Characterization of 6del heterozygous strains. a) Heterozygous genotypes for diploid strains YBS3992 and YBS3995 (herein 3992 and 3995) in which WT genes and gene replacements are indicated. b) DNA content analysis by flow cytometry confirms that both 3992 and 3995 exhibit normal diploid DNA contents, compared to a haploid WT control strain YBS255 (also see Supplementary Fig. 2). c) Drop tests (1:10 dilutions shown) document similar growth of WT and 6del strains (3992 and 3995 shown) across the indicated temperatures.

defects or temperature sensitivities, at least in the presence of heterozygous deletions of *ELG1*, *CLN2*, and *RAD61*.

Prior studies identified limited instances of cohesin mutation suppression that involved either *rad61Δ*, *elg1Δ*, or *cln2Δ* (Maradeo and Skibbens 2009; Rowland *et al.* 2009; Sutani *et al.* 2009; Buskirk and Skibbens 2022; Choudhary *et al.* 2022; Singh and Skibbens 2024). To identify novel combinations of suppressor mutations that might support the viability of cells deleted for one or more essential genes, we sporulated and then dissected, each 3 times, 2 independent 6del strains (3992 and 3995). Each of the 6 genes resides on separate chromosomes in yeast, providing 64 possible combinations. Over the course of this study, 344 tetrads were dissected from which a potential of 1376 spores were analyzed for novel genetic combinations that support cell viability. The majority of spores were inviable (178 viable spores = 13% viability), consistent with Mendelian frequencies for the deletion of 3 essential genes. While inclusion of suppressor mutations is predicted to increase this frequency, spore viability is likely hampered by reduced Mcd1 levels due to *ECO1* and *PDS5* deletions (Buskirk and Skibbens 2022; Choudhary *et al.* 2022; Singh and Skibbens 2024). A complete listing of all possible genotypes is provided in Table 2. In the following sections, dissection and subsequent phenotypic analyses are presented for all resulting spores that specifically include deletions of either *ECO1*, *PDS5*, or *SCC3* (Tables 2 and 3). We then turn to the analysis of novel strains that contain deletions of 2 or more essential cohesin genes.

Requirements for *eco1Δ* cell viability

rad61Δ *is an obligate condition for* eco1Δ *cell viability*

ECO1 represents the first example of an essential gene deletion analysis in this study (Skibbens *et al.* 1999; Tóth *et al.* 1999). As previously published, *eco1Δ rad61Δ* cells are viable (Rowland *et al.* 2009; Sutani *et al.* 2009), but only within a fairly narrow temperature range (Maradeo and Skibbens 2010; Buskirk and Skibbens 2022). From the above dissections, we recovered 50 *eco1Δ* spores in various combinations with nonessential gene deletions (Table 2). All 50 *eco1Δ* spores, however, also contained *rad61Δ*, revealing that deletion of *RAD61* is obligatory for *eco1Δ* cell viability. Twelve of the *eco1Δ* cells harbored only the additional *rad61Δ* allele and these exhibited ts growth defects (data not shown), as expected for this genetic combination (Maradeo and Skibbens 2010; Buskirk and Skibbens 2022). Thus, *rad61Δ* is obligatory, but not sufficient, for full bypass of *eco1Δ* cell growth.

Interchangeability of cln2Δ *and* elg1Δ *for* eco1Δ *cell viability*

We further parsed *eco1Δ rad61Δ* spores to identify those that also harbored *kanMX6*, which marks the deletion of either *CLN2*, *ELG1*, or both. *cln2Δ* rescues *eco1Δ rad61Δ ts* cell growth defects (Buskirk and Skibbens 2022), but *elg1Δ* also suppresses *eco1-203* cell ts growth defects (Maradeo and Skibbens 2009, 2010; Parnas *et al.* 2009). It thus became important to test the extent to which

Downloaded from https://academic.oup.com/genetics/advance-article/doi/10.1093/genetics/iyaf107/8159691 by guest on 23 June 2025

Table 2. Summary of the number of viable spores recovered from 6del dissections (344 tetrads with 1376 spores dissected).

Genotypes					Number of spores
eco1	*PDS5*	*SCC3*	*WT*	*RAD61*	0
eco1	*PDS5*	*SCC3*	*WT*	*rad61*	12
eco1	*PDS5*	*SCC3*	KAN+	*RAD61*	0
eco1	*PDS5*	*scc3*	*WT*	*RAD61*	0
eco1	*pds5*	*SCC3*	*WT*	*RAD61*	0
eco1	*PDS5*	*SCC3*	KAN+	*rad61*	38
eco1	*PDS5*	*scc3*	*WT*	*rad61*	0
eco1	*pds5*	*SCC3*	*WT*	*rad61*	0
eco1	*PDS5*	*scc3*	KAN+	*RAD61*	0
eco1	*pds5*	*SCC3*	KAN+	*RAD61*	2
eco1	*pds5*	*scc3*	*WT*	*RAD61*	0
eco1	*PDS5*	*scc3*	KAN+	*rad61*	0
eco1	*pds5*	*SCC3*	KAN+	*rad61*	1
eco1	*pds5*	*scc3*	*WT*	*rad61*	0
eco1	*pds5*	*scc3*	KAN+	*RAD61*	0
eco1	*pds5*	*scc3*	KAN+	*rad61*	1*
ECO1	*PDS5*	*SCC3*	*WT*	*RAD61*	16
ECO1	*PDS5*	*SCC3*	*WT*	*rad61*	13
ECO1	*PDS5*	*SCC3*	KAN+	*RAD61*	41
ECO1	*PDS5*	*scc3*	*WT*	*RAD61*	0
ECO1	*pds5*	*SCC3*	*WT*	*RAD61*	0
ECO1	*PDS5*	*SCC3*	KAN+	*rad61*	46
ECO1	*PDS5*	*scc3*	*WT*	*rad61*	0
ECO1	*pds5*	*SCC3*	*WT*	*rad61*	0
ECO1	*PDS5*	*scc3*	KAN+	*RAD61*	0
ECO1	*pds5*	*SCC3*	KAN+	*RAD61*	4
ECO1	*pds5*	*scc3*	*WT*	*RAD61*	0
ECO1	*PDS5*	*scc3*	KAN+	*rad61*	0
ECO1	*pds5*	*SCC3*	KAN+	*rad61*	4
ECO1	*pds5*	*scc3*	*WT*	*rad61*	0
ECO1	*pds5*	*scc3*	KAN+	*RAD61*	0
ECO1	*pds5*	*scc3*	KAN+	*rad61*	0
		Total number of viable spores			178

WT genes and mutated (or gene replacements) as indicated. KAN+ strains contain either *elg1Δ*::*kanMX6*, *cln2Δ*::*kanMX6*, or both. See Table 3, heterozygous for *SCC3* and *kanMX6* (see Supplementary Fig. 3).
WT, WT strains such as YPH499 or YBS255 (see Table 1); KAN+, *kanMX6*-containing spores that grow on selective media plates that contain G418 (see Materials and methods).

Table 3. Identification of KAN+ spores.

HIS+	URA+	KAN+	KAN+	Viable spores
eco1	*rad61*	*elg1*	-	7
eco1	*rad61*	-	*cln2*	7
eco1	*rad61*	*elg1*	*cln2*	10
			Total	24

PCR results identify KAN+ spores that contain either *elg1Δ*::*kanMX6*, *cln2Δ*::*kanMX6*, or both. HIS+ spores contain *eco1Δ*::*HIS3*; URA+ spores contain *rad61Δ*::*URA3*.

elg1Δ could replace *cln2Δ* in rescuing *eco1Δ rad61Δ* ts cell growth defects. As a first step, we determined which KAN+ (containing *kanMX6*) cells were deleted of *CLN2*, *ELG1*, or both. To ensure sufficient power to obtain all combinations, 24 of the 38 *eco1Δ rad61Δ* KAN+ cells were selected at random and tested by PCR. Roughly equal numbers of genetic combinations were found for each of the 3 classes: 7 *eco1Δ rad61Δ cln2Δ* triple null cells, 7 *eco1Δ rad61Δ elg1Δ* triple null cells, and 10 *eco1Δ rad61Δ cln2Δ elg1Δ* quadruple null cells (Table 3). We then tested all 7 isolates of *eco1Δ rad61Δ elg1Δ* triple null cells (YBS strains 4245, 4248,4262, 4270, 4291, 4297, and 4304) for ts growth defects, compared to WT cells (YBS255). While all strains exhibited robust growth at 30°C, *eco1Δ rad61Δ elg1Δ* triple null cells were inviable (or exhibited severe growth defects) when placed at 37°C (Fig. 3). Thus, *elg1Δ* cannot substitute for *cln2Δ* in supporting *eco1Δ* cell viability.

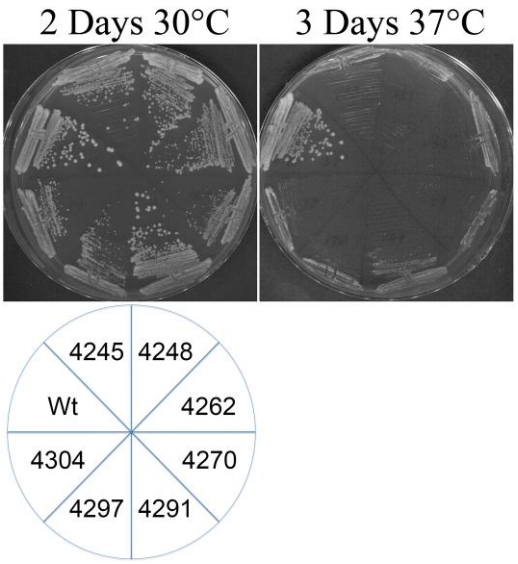

Fig. 3. Test for *elg1Δ*-dependent rescue of *eco1Δ rad61Δ* ts growth defects. WT and 7 independent isolates of *eco1Δ rad61Δ elg1Δ* triple null cells incubated at 30 or 37°C. YBS strain numbers (4245, 4248, 4262, 4270, 4291, 4297, and 4304) for *eco1Δ rad61Δ elg1Δ* triple null cells are shown.

Requirement for *pds5Δ* cell viability

We speculated, based on the suppression of *pds5-1* cell ts growth defects by either elevated *ECO1* expression (Noble *et al.* 2006) or deletion of *ELG1* (Maradeo and Skibbens 2010; Tong and Skibbens 2015), that *pds5Δ* cells might survive by some combination of suppressor mutations present in the 6del strains. The results show that cells deleted of *PDS5* required co-deletions of both *ELG1* and *CLN2*. No other gene deletions supported *pds5Δ* cell viability without those deletions (Table 2). These findings extend results obtained from prior genetic analyses (Psakhye and Branzei 2021; Choudhary *et al.* 2022) and reveal that separate pathways (*RAD61* for *eco1Δ* and *ELG1* for *pds5Δ*) are required to maintain cell viability and non-ts growth.

Requirement for *scc3Δ* cell viability

Losada and colleagues previously termed cohesin as a "chromatin engagement ring" (Remeseiro and Losada 2013). By extension, we posit that Smc1, Smc3, and Mcd1 form a "core" ring structure on top of which sits an auxiliary "bling" complex composed of Pds5, Scc3, and Rad61 (Fig. 1). To better understand the activities inherent to the core complex, it became important to identify spores deleted not only for *PDS5 and RAD61* but also for *SCC3*. *RAD61* is a nonessential gene, and *PDS5* deletion is fully compensated for by co-deletion of *ELG1* and *CLN2* (Table 2; Psakhye and Branzei 2021; Choudhary *et al.* 2022). Thus, we reasoned that deletion of the last remaining "bling" component SCC3 might similarly be compensated for by some combination of *ELG1*, *CLN2*, and *RAD61* deletions. Surprisingly, not a single *scc3Δ* spore was recovered from the 1,376 dissection products of our 6del strains (a single *NAT+* spore was confirmed by PCR to contain a WT copy of *SCC3*—see Supplementary Fig. 3). These results differentiate Scc3 from other bling components (Pds5 and Rad61) in terms of genetic mechanisms required to support cell viability.

Requirement of cells that harbor combinatorial deletions of essential genes

Prior studies suggest that Eco1 and Pds5 exhibit interdependent functions (Noble *et al.* 2006; Carretero *et al.* 2013; Chan *et al.* 2013;

Downloaded from https://academic.oup.com/genetics/advance-article/doi/10.1093/genetics/iyaf107/8156691 by guest on 23 June 2025

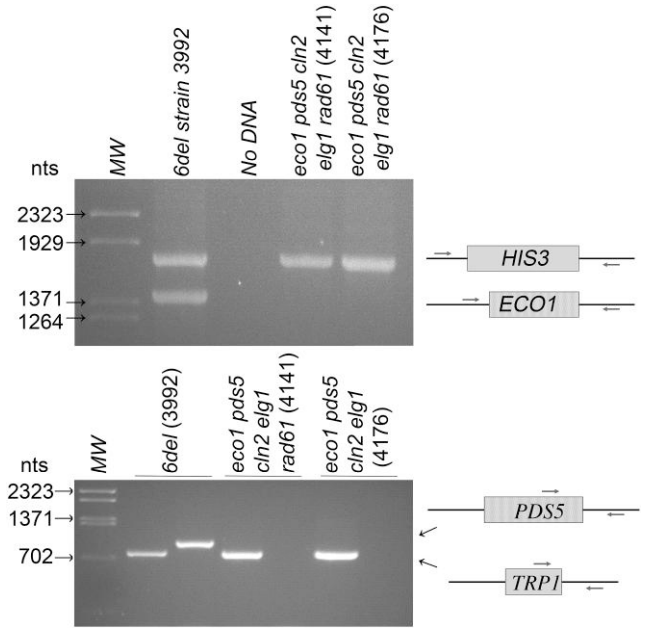

Fig. 4. PCR confirmation of *ECO1* and *PDS5* co-deletion in haploid spores recovered from 6del dissections. Top: A primer pair that flanks the *ECO1* open-reading frame produces 2 PCR products in the diploid 3992 6del strain. Retention of *ECO1* produces a 995nt PCR product while the homologous chromosome, in which *HIS3* replaces *ECO1*, produces a 1385nt PCR product. Only the 1385nt product is obtained from *eco1Δ pds5Δ rad61Δ elg1Δ cln2Δ* cells (strain 4141) and *eco1Δ pds5Δ elg1Δ cln2Δ* cells (strain 4176). Schematics at right illustrate primer positions, relative to the gene open-reading frames. Bottom: Primer pairs, specific to either *PDS5* or *TRP1*-replacement of *PDS5*, produced the expected PCR product sizes (984nts for *PDS5*, 812 nts for *TRP1*) in the 6del 3992 diploid strain. Only the 812nt product was obtained by PCR performed on *eco1Δ pds5Δ rad61Δ elg1Δ cln2Δ* cells (strain 4141) and *eco1Δ pds5Δ elg1Δ cln2Δ* cells (strain 4176). Schematics at right illustrate primer positions, relative to the gene open-reading frames.

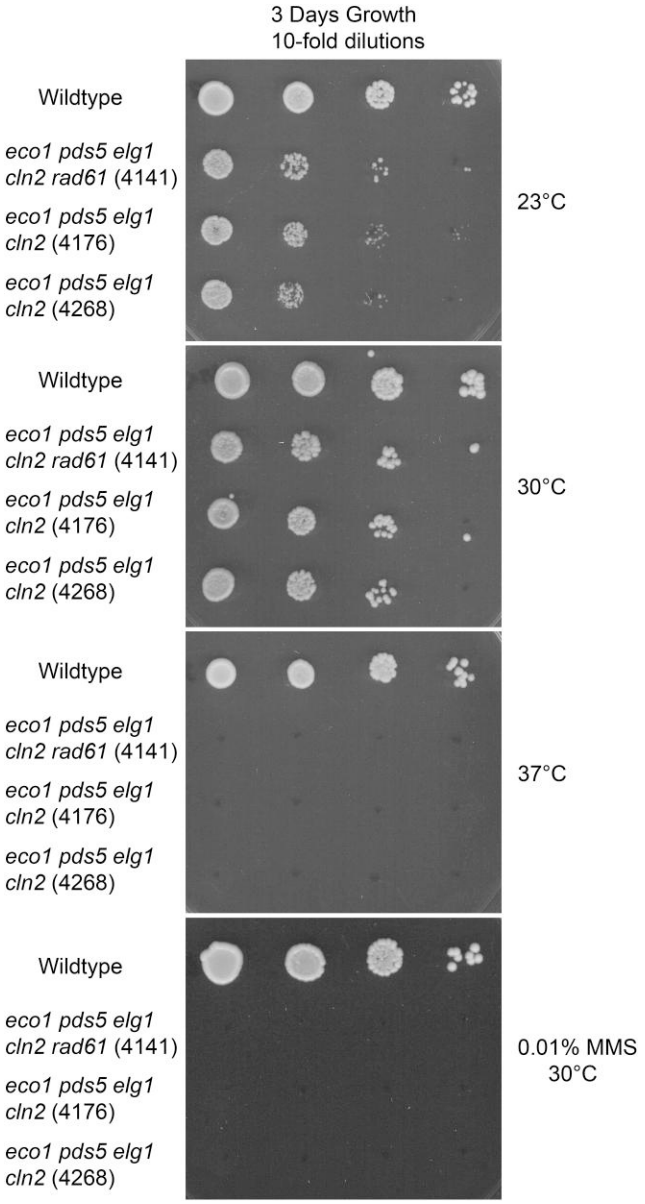

Fig. 5. Test for ts and genotoxic growth defects in spores that contain co-deletions of *ECO1* and *PDS5*. WT (YPH499), YBS4141 (*eco1Δ rad61Δ pds5Δ elg1Δ cln2Δ*), YBS4176 (*eco1Δ pds5Δ elg1Δ cln2Δ*), and YBS4268 (*eco1Δ pds5Δ elg1Δ cln2Δ*) are shown. Note that all 3 cohesin-mutated strains (4141, 4176, and 4268) exhibit both cold-sensitive growth defects (23°C), ts lethality (37°C), and genotoxic hypersensitivity upon exposure to MMS (0.01%) plates (30°C).

Tong and Skibbens 2014) such that *eco1Δ pds5Δ* spores produced from 6del strain dissections would be inviable. Conversely, deletion of *CLN2* is required for *pds5Δ elg1*Δ cell viability and rescues *eco1Δ rad61Δ* cell ts growth defects. It thus became important to test whether deletion of *CLN2*, in combination with other suppressors, might support co-deletion of both *ECO1* and *PDS5*. We indeed recovered 3 spores deleted for both *ECO1* and *PDS5*. One strain harbored deletions of all genes (except *scc3Δ*) pursued in this study: *eco1Δ*, *pds5Δ*, *elg1Δ*, *cln2Δ*, and *rad61Δ* (YBS4141, herein 4141). Surprisingly, 2 other *eco1Δ pds5Δ elg1Δ cln2Δ* spores (YBS4176 and YBS4268, herein 4176 and 4268) retained the WT copy of *RAD61*. We confirmed by PCR that both *eco1Δ* and *pds5Δ* loci were replaced by their respective markers (*HIS3* and *TRP1*) and that WT copies of both *ECO1* and *PDS5* were absent from these strains (Fig. 4).

Impact of *ECO1* and *PDS5* co-deletions on cell cycle progression

The generation of *eco1Δ pds5Δ elg1Δ cln2Δ* (with or without *rad61Δ*) cells is entirely unique. While exhibiting fairly robust growth at 30°C, all 3 strains grow slowly compared to WT cells (Supplementary Fig. 4) and exhibit severe ts lethality, cold-sensitive growth defects, and hypersensitivity to genotoxic agents (Fig. 5). The ts growth phenotype allowed for the characterization of cell cycle progression defects in cells that rely solely on Smc1, Smc3, Mcd1, and Scc3 cohesin subunits. It is well established that cohesin-mutated strains activate the spindle assembly checkpoint and exhibit a 2C bias (Skibbens *et al.* 1999; Tanaka *et al.* 2000; Hoque and Ishikawa 2002; Vagnarelli *et al.* 2004). Indeed, *eco1Δ pds5Δ elg1Δ cln2Δ* (with or without *rad61Δ*) cells, released from a preanaphase arrest (NZ), exhibited a mitotic exit defect, compared to WT cells, when released into fresh medium at 37°C (Supplementary Fig. 5). Prior studies linked cohesins, and cohesion establishment, to origins and prereplication complexes (Suter *et al.* 2004; Takahashi *et al.* 2004; Shimada and Gasser 2007; Guillou *et al.* 2010) Thus, we also tested for cell cycle progression defects by releasing cells, synchronized in early S phase (hydroxyurea, HU), into fresh 37°C medium. The results reveal that *eco1Δ pds5Δ elg1Δ cln2Δ* (with or without *rad61Δ*) cells progressed through S phase with kinetics nearly identical to that of WT cells (Supplementary Fig. 6).

Despite the fact that no prior studies report that cohesin-mutated cells exhibit a G1 exit defect, we tested for this possibility

Downloaded from https://academic.oup.com/genetics/advance-article/doi/10.1093/genetics/iyaf107/8159691 by guest on 23 June 2025

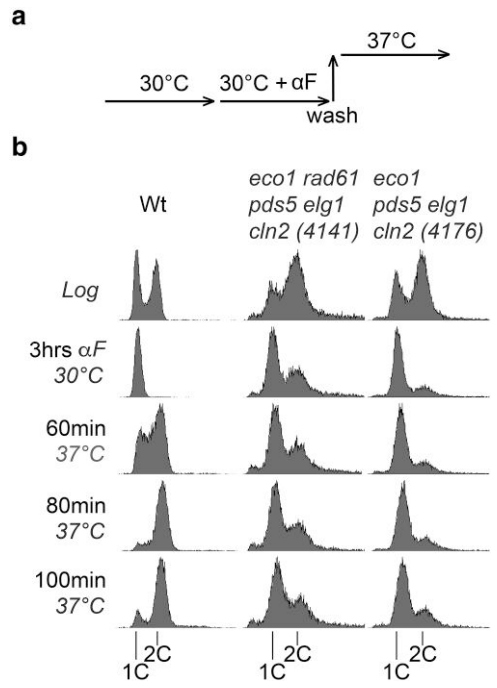

Fig. 6. Testing for G1/S transition defects in strains that include *ECO1* and *PDS5* co-deletions. a) Schematic outlining experimental protocol: log phase cultures were synchronized in G1 (αF, alpha factor) at the permissive temperature of 30°C prior to release into fresh 37°C medium. b) DNA profiles obtained using flow cytometry reveal that *eco1Δ pds5Δ cln2Δ elg1Δ rad61Δ* (strain 4141) and *eco1Δ pds5Δ cln2Δ elg1Δ* (strain 4176) fail to exit G1 or progress into S phase, compared to WT cells.

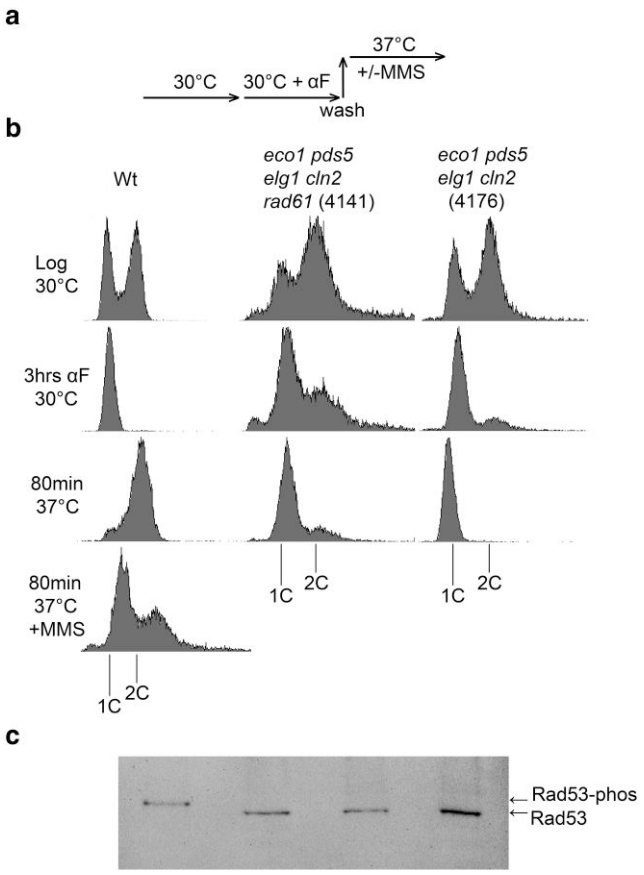

Fig. 7. The G1/S transition defect is not due to DNA damage checkpoint activation. a) Schematic outlining experimental protocol: log phase cultures were synchronized in the G1-phase (αF, alpha factor), prior to release into fresh 37°C medium. The WT culture was split into 2 with one exposed to MMS (0.1%) upon release into fresh 37°C medium. b) DNA profiles (flow cytometry) of WT, *eco1Δ pds5Δ cln2Δ elg1Δ rad61Δ* (strain 4141), and *eco1Δ pds5Δ cln2Δ elg1Δ* (strain 4176) cells over the experimental procedure. Note the inability of 4141 and 4269 to progress beyond G1 after 80 min outgrowth at 37°C, compared to WT cells. c) Western blot analysis of cells shown in b). Extracts from WT, 4141, and 4176 cells exhibit identical migration of Rad53. Only WT cells treated with MMS exhibit reduced Rad53 migration, an indication of DNA damage checkpoint activation.

as well. Log phase cultures of WT, *eco1Δ pds5Δ elg1Δ cln2Δ rad61Δ* (4141), and *eco1Δ pds5Δ elg1Δ cln2Δ* (4176) were washed, suspended in 30°C rich medium supplemented with alpha factor (αF) to synchronize the cultures in G1, then washed and released into 37°C fresh medium (Fig. 6a). WT and *eco1Δ pds5Δ elg1Δ cln2Δ* cells (4176) exhibited clear 1C peaks, while *eco1Δ pds5Δ elg1Δ cln2Δ rad61Δ* cells (4141), which appeared slow to fully synchronize, still achieved a predominantly 1C peak. Upon release from alpha factor, WT cells quickly progressed through S phase and into a predominantly 2C state. In contrast, neither of the 2 mutated strains progressed through the G1/S transition—retaining well-defined 1C peaks identical to those obtained in response to the alpha factor arrest (Fig. 6b). Cln2, as a G1 CDK component, promotes the G1/S transition, but the redundancy of G1 cyclins (Cln1, Cln2, and Cln3) requires combinatorial deletions to achieve a 1C arrest (Hadwiger *et al.* 1989; Richardson *et al.* 1989; Lew *et al.* 1992). We confirmed that *cln2Δ* single mutant strains efficiently navigate the G1/S transition (Supplementary Fig. 7) and that all cohesin-mutated strains retain both *CLN1* and *CLN3* (data not shown).

To our knowledge, this is the first report of a G1/S transition defect in strains that contain cohesin mutations. Prior results indicate that *eco1*-mutated cells exhibit increased reactive oxygen species (Mfarej and Skibbens 2020, 2022) and genotoxic hypersensitivity (Madril *et al.* 2001; Sjögren and Nasmyth 2001; Ström *et al.* 2007; Unal *et al.* 2007; van der Lelij *et al.* 2009). We decided to monitor Rad53 hyperphosphorylation to test whether the G1/S transition defect might be due to a DNA damage checkpoint (Pellicioli and Foiani 2005; Bacal *et al.* 2018). Log phase cultures of WT, *eco1Δ pds5Δ elg1Δ cln2Δ rad61Δ* (4141), and *eco1Δ pds5Δ elg1Δ cln2Δ* (4176) cells were washed, suspended in 30°C rich medium supplemented with alpha factor (αF), and then released at 37°C in fresh medium (Fig. 7a). As a positive control to induce Rad53 phosphorylation, the WT culture was divided into 2 and MMS added to a final concentration of 0.1% into one of the cultures. After 80 min of growth at 37°C, samples were harvested to assess DNA content (Fig. 7b) and Rad53 phosphorylation (Fig. 7c). As expected, WT cells quickly progressed out of G1 to achieve a predominantly 2C state while the mutated cells appeared to further consolidate into a G1 state with a 1C peak. WT cells treated with MMS, however, were significantly delayed in exiting G1, consistent with the DNA damage produced upon MMS exposure (Fig. 7b). As expected, MMS exposure produced a significant shift in Rad53 migration (Fig. 7c). In the absence of MMS treatment, all mutated strains exhibited the same rate of Rad53 migration as untreated WT cells (Fig. 7c). These findings reveal that some combination of deletions in these strains produce a severe G1/S transition defect that occurs independent of Rad53 phosphorylation.

Prior studies revealed that Mcd1 protein levels are low in tissue culture cells depleted of Pds5 or yeast cells co-deleted for either *PDS5* and *ELG1* or *ECO1* and *RAD61* (Psakhye and Branzei 2021; Choudhary *et al.* 2022; Singh and Skibbens 2024). Importantly,

Downloaded from https://academic.oup.com/genetics/advance-article/doi/10.1093/genetics/iyaf107/8159691 by guest on 23 June 2025

overexpressing *MCD1* is sufficient to rescue both *pds5Δ elg1Δ* lethality and *eco1Δ rad61Δ* ts lethality (Buskirk and Skibbens 2022; Choudhary *et al.* 2022; Singh and Skibbens 2024). We wondered whether elevated *MCD1* expression might rescue either the ts growth defects or the G1/S transition defects reported above (Figs. 5–7). We transformed into *eco1Δ pds5Δ elg1Δ cln2Δ rad61Δ* (4141) and *eco1Δ pds5Δ elg1Δ cln2Δ* (4176) strains either a 2μ *LEU2* plasmid (pRS425) or vector modified to include *MCD1* (pGS35), the latter of which we previously confirmed competent to rescue *mcd1-1*-mutated cells (Singh and Skibbens 2024). The resulting transformants were then grown on selective media plates at 30 and 37°C. Elevated *MCD1* expression failed to rescue the ts growth defects exhibited by either *eco1Δ pds5Δ elg1Δ cln2Δ rad61Δ* (4141) or *eco1Δ pds5Δ elg1Δ cln2Δ* (4176) strains (Supplementary Fig. 8). These findings do not preclude the possibility, however, that elevated *MCD1* expression might rescue the G1/S transition defect otherwise exhibited by these strains. Thus, log phase cultures of the transformed strains were synchronized in G1 (alpha factor, αF), washed and released into 37°C fresh medium as described above. Cell synchronization and progression through the cell cycle were monitored by flow cytometry. As expected, *eco1Δ pds5Δ elg1Δ cln2Δ rad61Δ* (4141) and *eco1Δ pds5Δ elg1Δ cln2Δ* (4176) strains that harbored the control 2μ *LEU2* plasmid failed to exit G1 (Supplementary Fig. 8). Elevated expression of *MCD1* also failed to rescue the G1/S transition defect.

Impact of *ECO1* and *PDS5* co-deletion on chromosome condensation

Cells mutated for either *ECO1* or *PDS5* exhibit chromosome condensation defects (Skibbens *et al.* 1999; Hartman *et al* 2000). Deletion of *RAD61*, however, rescues the condensation defects in either single-mutated cells (Guacci and Koshland 2012; Tong and Skibbens 2015; Buskirk and Skibbens 2022). To test the extent to which our mutated strains exhibit condensation defects, we pursued a streamlined strategy that produces quantifiable data on chromosome condensation in the absence of GFP, stacked antibody complexes, or probe hybridization (Shen and Skibbens 2017, 2020). Log phase cultures of WT, *eco1Δ pds5Δ elg1Δ cln2Δ rad61Δ* (4141), *eco1Δ pds5Δ elg1Δ cln2Δ* (4176), and *eco1Δ pds5Δ elg1Δ cln2Δ* (4268) cells were arrested in S phase (HU), washed, and then shifted to 37°C to medium supplemented with NZ to arrest cells in preanaphase (Fig. 8a). Following this regimen, we were able to obtain cultures with predominantly 2C peaks (Fig. 8b). Samples were then assessed for the stereotypical changes that occur at the rDNA locus, which transition from diffuse puff-like structures during G_1 to discrete loop-like structures during mitosis (Guacci *et al.* 1994, 1997; Lavoie *et al.* 2004; Guacci and Koshland 2012; Shen and Skibbens 2017, 2020). As expected, WT cells exhibited distinct rDNA loops that were easily discernible from the DNA mass (Fig. 8c and d). In comparison, *eco1Δ pds5Δ elg1Δ cln2Δ* and *eco1Δ pds5Δ elg1Δ cln2Δ rad61Δ* cells exhibited 2 distinct phenotypes. Predominantly, we observed hypercondensed chromatin and, when detectable, shortened rDNA loops. Thus, *rad61Δ* promotes a strong compensatory activity in which cohesin retention onto DNA produces highly condensed chromosomes and shortened rDNA loops in cells that harbor cohesin gene mutations (Guacci *et al.* 1997; Skibbens *et al.* 1999; Hartman *et al.* 2000; Gard *et al.* 2009; Bose *et al.* 2012; Guacci and Koshland 2012; Lopez-Serra *et al.* 2013; Orgil *et al.* 2015; Woodman *et al.* 2015; Buskirk and Skibbens 2022).

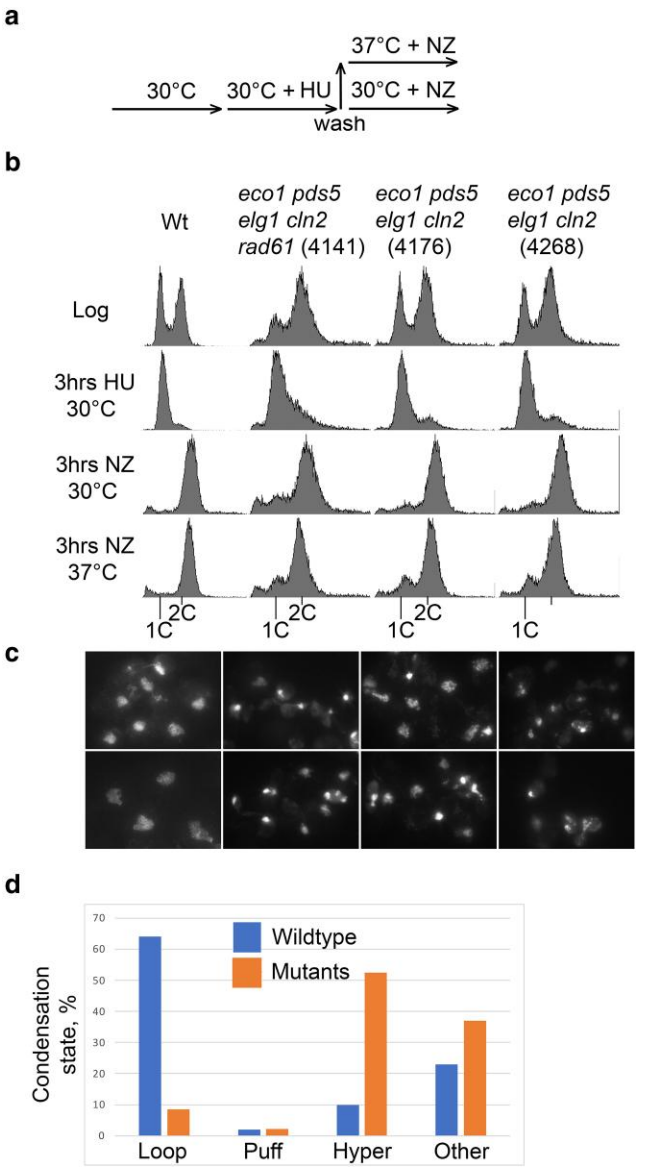

Fig. 8. Cells co-deleted for both *ECO1* and *PDS5* exhibit hypercondensed DNA. a) Schematic outlining experimental protocol: release of early S-phase-synchronized cells (HU, hydroxyurea) into 37°C medium supplemented with NZ to achieve a preanaphase arrest. b) Flow cytometer data of DNA content throughout the experiment. Log phase cultures were synchronized in early S phase (HU) at the permissive temperature and then released into fresh 37°C medium supplemented with NZ. c) Micrographs of DNA masses, aligned directly under the corresponding DNA profile and genotype. Chromosomal mass and rDNA loop structures were detected using DAPI. WT cells exhibit well-defined rDNA loops that often occur outside of the gyred DNA masses. In contrast, *eco1Δ pds5Δ elg1Δ cln2Δ rad61Δ* cells (4141) and *eco1Δ pds5Δ elg1Δ cln2Δ* (4176) cells exhibit hypercondensed DNA masses in which rDNA loops are rarely detectable. d) Quantification of loops and hypercondensed DNA masses. Few if any double rDNA rings were observed in either WT or mutant strains (data not shown). DNA masses with less condensed DNA masses, but in which rDNA loops were still not detected, are denoted as "other."

Discussion

Given the extensive roles that cohesins play in chromatin organization, elucidating the mechanisms through which cohesins are regulated remains at the forefront of cell and developmental research. Eco1 (human EFO1/ESCO1, EFO2/ESCO2) represents an essential family of acetyltransferases that regulate cohesins

Downloaded from https://academic.oup.com/genetics/advance-article/doi/10.1093/genetics/iyaf107/8159691 by guest on 23 June 2025

through Smc3 acetylation (Skibbens *et al.* 1999; Tóth *et al.* 1999; Bellows *et al.* 2003; Hou and Zou 2005; Vega *et al.* 2005; Rolef Ben-Shahar *et al.* 2008; Unal *et al.* 2008; Zhang *et al.* 2008). One of the key findings of the current study is the limited mechanisms through which Eco1 function can be bypassed. While numerous genetic manipulations (including *elg1Δ*, *cln2Δ*, elevated levels of either PCNA, Mms1, or Rtt101) partially suppress *eco1* mutant cell ts growth defects (Skibbens *et al.* 1999; Maradeo and Skibbens 2009; Zhang *et al.* 2017; Buskirk and Skibbens 2022), none individually support the viability of *eco1Δ* cells. Even the combination of suppressors (*cln2Δ* and *elg1Δ*) fails to support *eco1Δ* cell viability (current study). Instead, our findings document that *rad61Δ* is uniquely obligatory for *eco1Δ* cell viability of the genes tested.

A second revelation of the current study arises from the genetic relationships between Eco1 and Pds5. Unlike the acetyltransferase Eco1, Pds5 can associate stably with the cohesin complex. Despite this difference, there are surprising commonalities. First, both *pds5Δ* and *eco1Δ* cell growth depends in part on *CLN2* deletion (or increased Mcd1 levels) (Psakhye and Branzei 2021; Buskirk and Skibbens 2022; Choudhary *et al.* 2022; Singh and Skibbens 2024). Second, *pds5* and *eco1* cell ts growth defects are both suppressed by *elg1Δ* and also by elevated expression of PCNA/*POL30* (Skibbens *et al.* 1999; Maradeo and Skibbens 2009; Parnas *et al.* 2009; Tong and Skibbens 2015). Notably, *elg1Δ* greatly exacerbates the ts growth defects of *mcd1*-mutated cells (Maradeo and Skibbens 2009). Thus, cells with reduced Pds5 or Eco1 activities both benefit from elevated PCNA retention onto DNA, in contrast to the adverse impact on cells with reduced core cohesin function. The rescue of *pds5Δ* cells by *elg1Δ cln2Δ*, compared to the rescue of *eco1Δ* cells by *rad61Δ*, highlights the distinct mechanisms through which these 2 factors function (Tong and Skibbens 2014, 2015).

Scc3 comprises an auxiliary complex that, along with Pds5 and Rad61, can be biochemically enriched independent of the core cohesin ring complex (Rowland *et al.* 2009; Sutani *et al.* 2009). Because *RAD61* and *PDS5* can both be deleted, the latter requiring either co-deletion of *ELG1* and *CLN2* or expression of a chain-deficient SUMO/Smt3 allele (Psakhye and Branzei 2021; Choudhary *et al.* 2022), one might predict that some combination of suppressor mutations tested here would support *scc3Δ* cell viability. The inability to recover a single *scc3Δ* spore instead suggests that Scc3 plays a critical role beyond that of either Pds5 or Rad61. We note prior findings that Scc3 may play a structural role in cohesion, possibly by bridging together 2 or more cohesin complexes (Zhang and Pati 2009; Skibbens 2016; Xiang and Koshland 2021) or instead by promoting Scc2, Scc4-dependent loading of cohesins onto DNA (Orgil *et al.* 2015; Pathania *et al.* 2021; Psakhye and Branzei 2021; Collier and Nasmyth 2022; and see Fig. 9).

The generation of cells co-deleted for *ECO1* and *PDS5* is entirely unique. The genetic combinations required to support these cell viabilities are instructive. For instance, *cln2Δ* in part supports the viability of cells deleted for either *ECO1* or *PDS5*. Cln2 is a component of a CDK that impacts Mcd1 levels (Buskirk and Skibbens 2022; Choudhary *et al.* 2022; Singh and Skibbens 2024), but the exact mechanism remains to be fully elucidated. Notably, elevated expression of *MCD1* failed to rescue the ts growth defects of cells co-deleted for *ECO1* and *PDS5*. Thus, the deficit of these cells occurs independent of Mcd1 regulation. Deletion of *ELG1* is the second genetic component such that all *eco1Δ pds5Δ* cells recovered in the current study contain both *cln2Δ* and *elg1Δ* (Table 2). Elg1 is part of an RFC complex that unloads PCNA from the DNA replication fork. PCNA recruits Eco1 to the fork such that either elevated PCNA levels or *ELG1* deletion (which results in increased PCNA retention) suppress the growth defects

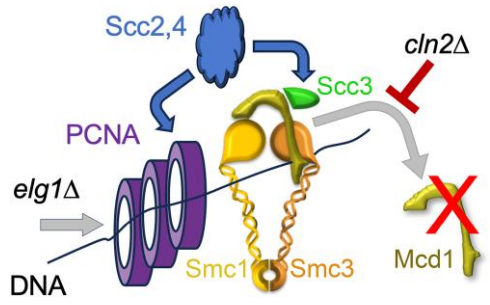

Fig. 9. Schematic illustrating mechanisms required to support the viability of cells deleted of *ECO1*, *PDS5*, *ELG1*, and *CLN2*. Cohesin complex composed of Smc1, Smc3, Mcd1, and Scc3 shown in the process of DNA replication (DNA fork not shown). Deletion of *ELG1* promotes elevated retention of PCNA onto DNA which, in turn, recruits the cohesin loading complex (Scc2,4 in blue). Scc3 (green) recruits Scc2,4 to facilitate cohesin deposition onto replicating DNA (black strand). Cells depleted of Eco1 or Pds5 exhibit reduced Mcd1 levels, a deficit rectified by *CLN2* deletion. See text for details.

otherwise exhibited by cells deficient in Eco1 function (Skibbens *et al.* 1999; Maradeo and Skibbens 2009; Parnas *et al.* 2009). The requirement by *eco1Δ pds5Δ* cells on *elg1Δ* may appear surprising given that elevated retention of chromatin-bound PCNA can no longer recruit Eco1. Recent findings, however, document that PCNA also recruits the deposition factor Scc2 (Psakhye *et al.* 2023; see Fig. 9). Note that PCNA-dependent co-recruitment of both Scc2 (cohesin loading) and Eco1 (cohesin stabilization) to the DNA replication fork satisfies all steps required for cohesion establishment (Skibbens 2000).

A further surprise of the current study was that deletion of *RAD61* appeared inconsequential to *eco1Δ pds5Δ elg1Δ cln2Δ* cells —despite analyses that *rad61Δ* is obligatory for *eco1Δ* cell survival. These findings provide both genetic and in vivo support for numerous studies that Pds5 is required for the recruitment of Rad61 to the cohesin core (Gandhi *et al.* 2006; Rowland *et al.* 2009; Shintomi and Hirano 2009; Kulemzina *et al.* 2012). In this scenario, deletion of *PDS5* phenocopies in part the deletion of *RAD61*—enabling the viability of cells deleted of *ECO1*. Regardless, the absence of Rad61 appears to be a common denominator for cells, that otherwise harbor cohesin mutations, in promoting chromatin hypercondensation (Lopez-Serra *et al.* 2013; Tong and Skibbens 2015; Shen and Skibbens 2017, 2020; Buskirk and Skibbens 2022; current study).

The final revelation of the current study is the discovery of a novel G1/S transition defect. The inability of *eco1Δ pds5Δ elg1Δ cln2Δ* cells (with or without *RAD61*) to progress through the G1/S transition, or START, is surprising given that no single gene deletion exhibits a G1/S transition defect (Skibbens *et al.* 1999; Panizza *et al.* 2000; Guacci and Koshland 2012). A 10 min delay during DNA replication was previously noted for *eco1* ts cells (Guacci and Koshland 2012), but a similar delay in S progression was not detected in *eco1Δ pds5Δ elg1Δ cln2Δ* cells (with or without *RAD61*) in the current study. The exact genetic combination required to elicit this G1/S transition defect remains unknown, but current results do not support a DNA damage checkpoint-based mechanism. Nor do we find evidence that the delay involves reduced Mcd1 levels. The extent to which cohesins promote the activities of the other G1 CDKs through a transcriptional mechanism thus requires further exploration. For instance, HeLa cells reduced for RAD21 (human homolog of Mcd1) exhibit an extended cell cycle that is alleviated by c-Myc expression (Rohban *et al.* 2017).

Downloaded from https://academic.oup.com/genetics/advance-article/doi/10.1093/genetics/iyaf107/8159691 by guest on 23 June 2025

Data availability

Strains and plasmids are available upon request. The authors affirm that all data necessary for confirming the conclusions of the article are present within the article, figures, and tables.

Supplemental material available at GENETICS online.

Acknowledgments

The authors thank past and present Skibbens lab members (Gurvir Singh, Brandon Nguyen, Maia Pohlhaus, Abbie Brown, Fiona Mensching, MJ Schwab, and Niusha Banoukh) and the Yeast Super Group meeting members for the helpful discussions throughout the course of this study. The authors are especially grateful to Gurvir Singh for the careful editing of the manuscript.

Funding

This work was supported by an award to R.V.S. from the National Institutes of Health (R15GM139097). Any opinions, findings, and conclusions or recommendations expressed in this study are those of the authors and do not necessarily reflect the views of the National Institutes of Health.

Conflicts of interest

The authors declare no conflicts of interest.

Literature cited

Arbel M, Choudhary K, Tfilin O, Kupiec M. 2021. PCNA loaders and unloaders-one ring that rules them all. Genes (Basel). 12(11): 1812. doi:10.3390/genes12111812.

Bacal J, Moriel-Carretero M, Pardo B, Barthe A, Sharma S, Chabes A, Lengronne A, Pasero P. 2018. Mrc1 and Rad9 cooperate to regulate initiation and elongation of DNA replication in response to DNA damage. EMBO J. 37(21):e99319. doi:10.15252/embj.201899319.

Barton RE, Massari LF, Robertson D, Marston AL. 2022. Eco1-dependent cohesin acetylation anchors chromatin loops and cohesion to define functional meiotic chromosome domains. Elife. 11:e74447. doi:10.7554/eLife.74447.

Bellows AM, Kenna MA, Cassimeris L, Skibbens RV. 2003. Human EFO1p exhibits acetyltransferase activity and is a unique combination of linker histone and Ctf7p/Eco1p chromatid cohesion establishment domains. Nucleic Acids Res. 31(21):6334–6343. doi: 10.1093/nar/gkg811.

Bender D, Da Silva EML, Chen J, Poss A, Gawey L, Rulon Z, Rankin S. 2020. Multivalent interaction of ESCO2 with the replication machinery is required for sister chromatid cohesion in vertebrates. Proc Natl Acad Sci U S A. 117(2):1081–1089. doi:10.1073/pnas.1911936117.

Birchler JA, Veitia RA. 2021. One hundred years of gene balance: how stoichiometric issues affect gene expression, genome evolution, and quantitative traits. Cytogenet Genome Res. 161(10-11): 529–550. doi:10.1159/000519592.

Bose T, Lee KK, Lu S, Xu B, Harris B, Slaughter B, Unruh J, Garrett A, McDowell W, Box A, *et al.* 2012. Cohesin proteins promote ribosomal RNA production and protein translation in yeast and human cells. PLoS Genet. 8(6):e1002749. doi:10.1371/journal.pgen.1002749.

Buskirk S, Skibbens RV. 2022. G1-Cyclin2 (Cln2) promotes chromosome hypercondensation in eco1/ctf7 rad61 null cells during hyperthermic stress in Saccharomyces cerevisiae. G3 (Bethesda). 12(8):jkac157. doi:10.1093/g3journal/jkac157.

Carretero M, Ruiz-Torres M, Rodríguez-Corsino M, Barthelemy I, Losada A. 2013. Pds5B is required for cohesion establishment and Aurora B accumulation at centromeres. EMBO J. 32(22): 2938–2949. doi:10.1038/emboj.2013.230.

Chan KL, Gligoris T, Upcher W, Kato Y, Shirahige K, Nasmyth K, Beckouët F. 2013. Pds5 promotes and protects cohesin acetylation. Proc Natl Acad Sci U S A. 110(32):13020–13025. doi:10.1073/pnas.1306900110.

Chang LH, Noordermeer D. 2024. Permeable TAD boundaries and their impact on genome-associated functions. Bioessays. 46(10): e2400137. doi:10.1002/bies.202400137.

Choudhary K, Itzkovich Z, Alonso-Perez E, Bishara H, Dunn B, Sherlock G, Kupiec M. 2022. S. cerevisiae cells can grow without the Pds5 cohesin subunit. mBio. 13(4):e0142022. doi:10.1128/mbio.01420-22.

Chunduri NK, Barthel K, Storchova Z. 2022. Consequences of chromosome loss: why do cells need each chromosome twice? Cells. 11(9):1530. doi:10.3390/cells11091530.

Ciosk R, Shirayama M, Shevchenko A, Tanaka T, Toth A, Shevchenko A, Nasmyth K. 2000. Cohesin's binding to chromosomes depends on a separate complex consisting of Scc2 and Scc4 proteins. Mol Cell. 5(2):243–254. doi:10.1016/S1097-2765(00)80420-7.

Collier JE, Nasmyth KA. 2022. DNA passes through cohesin's hinge as well as its Smc3-kleisin interface. Elife. 11:e80310. doi:10.7554/eLife.80310.

Dauban L, Montagne R, Thierry A, Lazar-Stefanita L, Bastié N, Gadal O, Cournac A, Koszul R, Beckouët F. 2020. Regulation of cohesin-mediated chromosome folding by eco1 and other partners. Mol Cell. 77(6):1279–1293.e4. doi:10.1016/j.molcel.2020.01.019.

Fritz AJ, Sehgal N, Pliss A, Xu J, Berezney R. 2019. Chromosome territories and the global regulation of the genome. Genes Chromosomes Cancer. 58(7):407–426. doi:10.1002/gcc.22732.

Gandhi R, Gillespie PJ, Hirano T. 2006. Human Wapl is a cohesin-binding protein that promotes sister-chromatid resolution in mitotic prophase. Curr Biol. 16(24):2406–2417. doi:10.1016/j.cub.2006.10.061.

Gard S, Light W, Xiong B, Bose T, McNairn AJ, Harris B, Fleharty B, Seidel C, Brickner JH, Gerton JL. 2009. Cohesinopathy mutations disrupt the subnuclear organization of chromatin. J Cell Biol. 187(4):455–462. doi:10.1083/jcb.200906075.

Gerring SL, Spencer F, Hieter P. 1990. The CHL 1 (CTF 1) gene product of Saccharomyces cerevisiae is important for chromosome transmission and normal cell cycle progression in G2/M. EMBO J. 9(13): 4347–4358. doi:10.1002/j.1460-2075.1990.tb07884.x.

Golov AK, Gavrilov AA. 2024. Cohesin complex: structure and principles of interaction with DNA. Biochemistry (Mosc). 89(4):585–600. doi:10.1134/S0006297924040011.

Guacci V, Hogan E, Koshland D. 1994. Chromosome condensation and sister chromatid pairing in budding yeast. J Cell Biol. 125(3): 517–530. doi:10.1083/jcb.125.3.517.

Guacci V, Koshland D. 2012. Cohesin-independent segregation of sister chromatids in budding yeast. Mol Biol Cell. 23(4):729–739. doi: 10.1091/mbc.e11-08-0696.

Guacci V, Koshland D, Strunnikov A. 1997. A direct link between sister chromatid cohesion and chromosome condensation revealed through the analysis of MCD1 in S. cerevisiae. Cell. 91(1):47–57. doi:10.1016/S0092-8674(01)80008-8.

Guillou E, Ibarra A, Coulon V, Casado-Vela J, Rico D, Casal I, Schwob E, Losada A, Méndez J. 2010. Cohesin organizes chromatin loops at DNA replication factories. Genes Dev. 24(24):2812–2822. doi: 10.1101/gad.608210.

Hadwiger JA, Wittenberg C, Richardson HE, de Barros Lopes M, Reed SI. 1989. A family of cyclin homologs that control the G1 phase in

Downloaded from https://academic.oup.com/genetics/advance-article/doi/10.1093/genetics/iyaf107/8159691 by guest on 23 June 2025

yeast. Proc Natl Acad Sci U S A. 86(16):6255–6259. doi:10.1073/pnas.86.16.6255.
Hartman T, Stead K, Koshland D, Guacci V. 2000. Pds5p is an essential chromosomal protein required for both sister chromatid cohesion and condensation in Saccharomyces cerevisiae. J Cell Biol. 151(3):613–626. doi:10.1083/jcb.151.3.613.
Higashi TL, Ikeda M, Tanaka H, Nakagawa T, Bando M, Shirahige K, Kubota Y, Takisawa H, Masukata H, Takahashi TS. 2012. The pre-replication complex recruits XEco2 to chromatin to promote cohesin acetylation in Xenopus egg extracts. Curr Biol. 22(11):977–988. doi:10.1016/j.cub.2012.04.013.
Hoque MT, Ishikawa F. 2002. Cohesin defects lead to premature sister chromatid separation, kinetochore dysfunction, and spindle-assembly checkpoint activation. J Biol Chem. 277(44):42306–42314. doi:10.1074/jbc.M206836200.
Horsfield JA. 2023. Full circle: a brief history of cohesin and the regulation of gene expression. FEBS J. 290(7):1670–1687. doi:10.1111/febs.16362.
Hou F, Zou H. 2005. Two human orthologues of Eco1/Ctf7 acetyltransferases are both required for proper sister-chromatid cohesion. Mol Biol Cell. 16(8):3908–3918. doi:10.1091/mbc.e04-12-1063.
Ivanov D, Schleiffer A, Eisenhaber F, Mechtler K, Haering CH, Nasmyth K. 2002. Eco1 is a novel acetyltransferase that can acetylate proteins involved in cohesion. Curr Biol. 12(4):323–328. doi:10.1016/S0960-9822(02)00681-4.
Karpinska MA, Oudelaar AM. 2023. The role of loop extrusion in enhancer-mediated gene activation. Curr Opin Genet Dev. 79:102022. doi:10.1016/j.gde.2023.102022.
Kenna MA, Skibbens RV. 2003. Mechanical link between cohesion establishment and DNA replication: Ctf7p/Eco1p, a cohesion establishment factor, associates with three different replication factor C complexes. Mol Cell Biol. 23(8):2999–3007. doi:10.1128/MCB.23.8.2999-3007.2003.
Konecna M, Abbasi Sani S, Anger M. 2023. Separase and roads to disengage sister chromatids during anaphase. Int J Mol Sci. 24(5):4604. doi:10.3390/ijms24054604.
Kueng S, Hegemann B, Peters BH, Lipp JJ, Schleiffer A, Mechtler K, Peters JM. 2006. Wapl controls the dynamic association of cohesin with chromatin. Cell. 127(5):955–967. doi:10.1016/j.cell.2006.09.040.
Kulemzina I, Schumacher MR, Verma V, Reiter J, Metzler J, Failla AV, Lanz C, Sreedharan VT, Rätsch G, Ivanov D. 2012. Cohesin rings devoid of Scc3 and Pds5 maintain their stable association with the DNA. PLoS Genet. 8(8):e1002856. doi:10.1371/journal.pgen.1002856.
Kurlandzka A, Rytka J, Rózalska B, Wysocka M. 1999. Saccharomyces cerevisiae IRR1 protein is indirectly involved in colony formation. Yeast. 15(1):23–33. doi:10.1002/(SICI)1097-0061(19990115)15:1<23:AID-YEA337>3.0.CO;2-E.
Lavoie BD, Hogan E, Koshland D. 2004. In vivo requirements for rDNA chromosome condensation reveal two cell-cycle-regulated pathways for mitotic chromosome folding. Genes Dev. 18(1):76–87. doi:10.1101/gad.1150404.
Lew DJ, Marini NJ, Reed SI. 1992. Different G1 cyclins control the timing of cell cycle commitment in mother and daughter cells of the budding yeast S. cerevisiae. Cell. 69(2):317–327. doi:10.1016/0092-8674(92)90412-6.
Liyakat Ali TM, Brunet A, Collas P, Paulsen J. 2021. TAD cliques predict key features of chromatin organization. BMC Genomics. 22(1):499. doi:10.1186/s12864-021-07815-8.
Longtine MS, McKenzie A 3rd, Demarini DJ, Shah NG, Wach A, Brachat A, Philippsen P, Pringle JR. 1998. Additional modules for versatile and economical PCR-based gene deletion and modification in Saccharomyces cerevisiae. Yeast. 14(10):953–961. doi:10.1002/(SICI)1097-0061(199807)14:10<953::AID-YEA293>3.0.CO;2-U.
Lopez-Serra L, Lengronne A, Borges V, Kelly G, Uhlmann F. 2013. Budding yeast Wapl controls sister chromatid cohesion maintenance and chromosome condensation. Curr Biol. 23(1):64–69. doi:10.1016/j.cub.2012.11.030.
Luppino JM, Park DS, Nguyen SC, Lan Y, Xu Z, Yunker R, Joyce EF. 2020. Cohesin promotes stochastic domain intermingling to ensure proper regulation of boundary-proximal genes. Nat Genet. 52(8):840–848. doi:10.1038/s41588-020-0647-9.
Madril AC, Johnson RE, Washington MT, Prakash L, Prakash S. 2001. Fidelity and damage bypass ability of Schizosaccharomyces pombe Eso1 protein, comprised of DNA polymerase eta and sister chromatid cohesion protein Ctf7. J Biol Chem. 276(46):42857–-42862. doi:10.1074/jbc.M106917200.
Maradeo ME, Skibbens RV. 2009. The Elg1-RFC clamp-loading complex performs a role in sister chromatid cohesion. PLoS One. 4(3):e4707. doi:10.1371/journal.pone.0004707.
Maradeo ME, Skibbens RV. 2010. Replication factor C complexes play unique pro- and anti-establishment roles in sister chromatid cohesion. PLoS One. 5(10):e15381. doi:10.1371/journal.pone.0015381.
McAinsh AD, Kops GJPL. 2023. Principles and dynamics of spindle assembly checkpoint signalling. Nat Rev Mol Cell Biol. 24(8):543–559. doi:10.1038/s41580-023-00593-z.
Mfarej MG, Skibbens RV. 2020. DNA damage induces Yap5-dependent transcription of ECO1/CTF7 in Saccharomyces cerevisiae. PLoS One. 15(12):e0242968. doi:10.1371/journal.pone.0242968.
Mfarej MG, Skibbens RV. 2022. Genetically induced redox stress occurs in a yeast model for Roberts syndrome. G3 (Bethesda). 12(2):jkab426. doi:10.1093/g3journal/jkab426.
Michaelis C, Ciosk R, Nasmyth K. 1997. Cohesins: chromosomal proteins that prevent premature separation of sister chromatids. Cell. 91(1):35–45. doi:10.1016/S0092-8674(01)80007-6.
Moldovan GL, Pfander B, Jentsch S. 2006. PCNA controls establishment of sister chromatid cohesion during S phase. Mol Cell. 23(5):723–732. doi:10.1016/j.molcel.2006.07.007.
Nishiyama T. 2019. Cohesion and cohesin-dependent chromatin organization. Curr Opin Cell Biol. 58:8–14. doi:10.1016/j.ceb.2018.11.006.
Noble D, Kenna MA, Dix M, Skibbens RV, Unal E, Guacci V. 2006. Intersection between the regulators of sister chromatid cohesion establishment and maintenance in budding yeast indicates a multi-step mechanism. Cell Cycle. 5(21):2528–2536. doi:10.4161/cc.5.21.3405.
Orgil O, Matityahu A, Eng T, Guacci V, Koshland D, Onn I. 2015. A conserved domain in the scc3 subunit of cohesin mediates the interaction with both mcd1 and the cohesin loader complex. PLoS Genet. 11(3):e1005036. doi:10.1371/journal.pgen.1005036.
Panizza S, Tanaka T, Hochwagen A, Eisenhaber F, Nasmyth K. 2000. Pds5 cooperates with cohesin in maintaining sister chromatid cohesion. Curr Biol. 10(24):1557–1564. doi:10.1016/S0960-9822(00)00854-X.
Parnas O, Zipin-Roitman A, Mazor Y, Liefshitz B, Ben-Aroya S, Kupiec M. 2009. The ELG1 clamp loader plays a role in sister chromatid cohesion. PLoS One. 4(5):e5497. doi:10.1371/journal.pone.0005497.
Pathania A, Liu W, Matityahu A, Irudayaraj J, Onn I. 2021. Chromosome loading of cohesin depends on conserved residues in Scc3. Curr Genet. 67(3):447–459. doi:10.1007/s00294-020-01150-3.
Pellicioli A, Foiani M. 2005. Signal transduction: how rad53 kinase is activated. Curr Biol. 15(18):R769–R771. doi:10.1016/j.cub.2005.08.057.
Psakhye I, Branzei D. 2021. SMC complexes are guarded by the SUMO protease Ulp2 against SUMO-chain-mediated turnover. Cell Rep. 36(5):109485. doi:10.1016/j.celrep.2021.109485.
Psakhye I, Kawasumi R, Abe T, Hirota K, Branzei D. 2023. PCNA recruits cohesin loader Scc2 to ensure sister chromatid cohesion.

Downloaded from https://academic.oup.com/genetics/advance-article/doi/10.1093/genetics/iyaf107/8159691 by guest on 23 June 2025

Nat Struct Mol Biol. 30(9):1286–1294. doi:10.1038/s41594-023-01064-x.
Remeseiro S, Losada A. 2013. Cohesin, a chromatin engagement ring. Curr Opin Cell Biol. 25(1):63–71. doi:10.1016/j.ceb.2012.10.013.
Richardson HE, Wittenberg C, Cross F, Reed SI. 1989. An essential G1 function for cyclin-like proteins in yeast. Cell. 59(6):1127–1133. doi:10.1016/0092-8674(89)90768-X.
Rohban S, Cerutti A, Morelli MJ, d'Adda di Fagagna F, Campaner S. 2017. The cohesin complex prevents Myc-induced replication stress. Cell Death Dis. 8(7):e2956. doi:10.1038/cddis.2017.345.
Rolef Ben-Shahar T, Heeger S, Lehane C, East P, Flynn H, Skehel M, Uhlmann F. 2008. Eco1-dependent cohesin acetylation during establishment of sister chromatid cohesion. Science. 321(5888):563–566. doi:10.1126/science.1157774.
Rollins RA, Korom M, Aulner N, Martens A, Dorsett D. 2004. Drosophila nipped-B protein supports sister chromatid cohesion and opposes the stromalin/Scc3 cohesion factor to facilitate long-range activation of the cut gene. Mol Cell Biol. 24(8):3100–3111. doi:10.1128/MCB.24.8.3100-3111.2004.
Rowland BD, Roig MB, Nishino T, Kurze A, Uluocak P, Mishra A, Beckouët F, Underwood P, Metson J, Imre R, *et al.* 2009. Building sister chromatid cohesion: smc3 acetylation counteracts an antiestablishment activity. Mol Cell. 33(6):763–774. doi:10.1016/j.molcel.2009.02.028.
Shen D, Skibbens RV. 2017. Temperature-dependent regulation of rDNA condensation in Saccharomyces cerevisiae. Cell Cycle. 16(11):1118–1127. doi:10.1080/15384101.2017.1317409.
Shen D, Skibbens RV. 2020. Promotion of hyperthermic-induced rDNA hypercondensation in Saccharomyces cerevisiae. Genetics. 214(3):589–604. doi:10.1534/genetics.119.302994.
Shimada K, Gasser SM. 2007. The origin recognition complex functions in sister-chromatid cohesion in Saccharomyces cerevisiae. Cell. 128(1):85–99. doi:10.1016/j.cell.2006.11.045.
Shintomi K, Hirano T. 2009. Releasing cohesin from chromosome arms in early mitosis: opposing actions of Wapl-Pds5 and Sgo1. Genes Dev. 23(18):2224–2236. doi:10.1101/gad.1844309.
Shiomi Y, Nishitani H. 2017. Control of genome integrity by RFC complexes; conductors of PCNA loading onto and unloading from chromatin during DNA replication. Genes (Basel). 8(2):52. doi:10.3390/genes8020052.
Sikorski RS, Hieter P. 1989. A system of shuttle vectors and yeast host strains designed for efficient manipulation of DNA in *Saccharomyces cerevisae*. Genetics. 122(1):19–27. doi:10.1093/genetics/122.1.19.
Singh G, Skibbens RV. 2024. Fdo1, Fkh1, Fkh2and the Swi6-Mbp1 MBF complex regulate Mcd1 levels to impact eco1 rad61 cell growth in Saccharomyces cerevisiae. Genetics. 228(2):iyae128. doi:10.1093/genetics/iyae128.
Sjögren C, Nasmyth K. 2001. Sister chromatid cohesion is required for postreplicative double-strand break repair in Saccharomyces cerevisiae. Curr Biol. 11(12):991–995. doi:10.1016/S0960-9822(01)00271-8.
Skibbens RV. 2000. Holding your own: establishing sister chromatid cohesion. Genome Res. 10(11):1664–1671. doi:10.1101/gr.153600.
Skibbens RV. 2016. Of rings and rods: regulating cohesin entrapment of DNA to generate intra- and intermolecular tethers. PLoS Genet. 12(10):e1006337. doi:10.1371/journal.pgen.1006337.
Skibbens RV. 2019. Condensins and cohesins—one of these things is not like the other! J Cell Sci. 132(3):jcs220491. doi:10.1242/jcs.220491.
Skibbens RV, Corson LB, Koshland D, Hieter P. 1999. Ctf7p is essential for sister chromatid cohesion and links mitotic chromosome structure to the DNA replication machinery. Genes Dev. 13(3):307–319. doi:10.1101/gad.13.3.307.
Ström L, Karlsson C, Lindroos HB, Wedahl S, Katou Y, Shirahige K, Sjögren C. 2007. Postreplicative formation of cohesion is required for repair and induced by a single DNA break. Science. 317(5835):242–245. doi:10.1126/science.1140649.
Sutani T, Kawaguchi T, Kanno R, Itoh T, Shirahige K. 2009. Budding yeast Wpl1(Rad61)-Pds5 complex counteracts sister chromatid cohesion-establishing reaction. Curr Biol. 19(6):492–497. doi:10.1016/j.cub.2009.01.062.
Suter B, Tong A, Chang M, Yu L, Brown GW, Boone C, Rine J. 2004. The origin recognition complex links replication, sister chromatid cohesion and transcriptional silencing in Saccharomyces cerevisiae. Genetics. 167(2):579–591. doi:10.1534/genetics.103.024851.
Takahashi TS, Yiu P, Chou MF, Gygi S, Walter JC. 2004. Recruitment of Xenopus Scc2 and cohesin to chromatin requires the pre-replication complex. Nat Cell Biol. 6(10):991–996. doi:10.1038/ncb1177.
Tanaka K, Yonekawa T, Kawasaki Y, Kai M, Furuya K, Iwasaki M, Murakami H, Yanagida M, Okayama H. 2000. Fission yeast Eso1p is required for establishing sister chromatid cohesion during S phase. Mol Cell Biol. 20(10):3459–3469. doi:10.1128/MCB.20.10.3459-3469.2000.
Tedeschi A, Wutz G, Huet S, Jaritz M, Wuensche A, Schirghuber E, Davidson IF, Tang W, Cisneros DA, Bhaskara V, *et al.* 2013. Wapl is an essential regulator of chromatin structure and chromosome segregation. Nature. 501(7468):564–568. doi:10.1038/nature12471.
Tong K, Skibbens RV. 2014. Cohesin without cohesion: a novel role for Pds5 in Saccharomyces cerevisiae. PLoS One. 9(6):e100470. doi:10.1371/journal.pone.0100470.
Tong K, Skibbens RV. 2015. Pds5 regulators segregate cohesion and condensation pathways in Saccharomyces cerevisiae. Proc Natl Acad Sci U S A. 112(22):7021–7026. doi:10.1073/pnas.1501369112.
Tonkin ET, Wang TJ, Lisgo S, Bamshad MJ, Strachan T. 2004. NIPBL, encoding a homolog of fungal Scc2-type sister chromatid cohesion proteins and fly Nipped-B, is mutated in Cornelia de Lange syndrome. Nat Genet. 36(6):636–641. doi:10.1038/ng1363.
Tóth A, Ciosk R, Uhlmann F, Galova M, Schleiffer A, Nasmyth K. 1999. Yeast cohesin complex requires a conserved protein, Eco1p(Ctf7), to establish cohesion between sister chromatids during DNA replication. Genes Dev. 13(3):320–333. doi:10.1101/gad.13.3.320.
Unal E, Heidinger-Pauli JM, Kim W, Guacci V, Onn I, Gygi SP, Koshland DE. 2008. A molecular determinant for the establishment of sister chromatid cohesion. Science. 321(5888):566–569. doi:10.1126/science.1157880.
Unal E, Heidinger-Pauli JM, Koshland D. 2007. DNA double-strand breaks trigger genome-wide sister-chromatid cohesion through Eco1 (Ctf7). Science. 317(5835):245–248. doi:10.1126/science.1140637.
Vagnarelli P, Morrison C, Dodson H, Sonoda E, Takeda S, Earnshaw WC. 2004. Analysis of Scc1-deficient cells defines a key metaphase role of vertebrate cohesin in linking sister kinetochores. EMBO Rep. 5(2):167–171. doi:10.1038/sj.embor.7400077.
van der Lelij P, Godthelp BC, van Zon W, van Gosliga D, Oostra AB, Steltenpool J, de Groot J, Scheper RJ, Wolthuis RM, Waisfisz Q, *et al.* 2009. The cellular phenotype of Roberts syndrome fibroblasts as revealed by ectopic expression of ESCO2. PLoS One. 4(9):e6936. doi:10.1371/journal.pone.0006936.
van Schie JJ, de Lint K, Pai GM, Rooimans MA, Wolthuis RM, de Lange J. 2022. MMS22L-TONSL functions in sister chromatid cohesion in a pathway parallel to DSCC1-RFC. Life Sci Alliance. 6(2):e202201596. doi:10.26508/lsa.202201596.
Vega H, Waisfisz Q, Gordillo M, Sakai N, Yanagihara I, Yamada M, van Gosliga D, Kayserili H, Xu C, Ozono K, *et al.* 2005. Roberts syndrome is caused by mutations in ESCO2, a human homolog of

Downloaded from https://academic.oup.com/genetics/advance-article/doi/10.1093/genetics/iyaf107/8159691 by guest on 23 June 2025

yeast ECO1 that is essential for the establishment of sister chromatid cohesion. Nat Genet. 37(5):468–470. doi:10.1038/ng1548.

Watrin E, Schleiffer A, Tanaka K, Eisenhaber F, Nasmyth K, Peters JM. 2006. Human Scc4 is required for cohesin binding to chromatin, sister-chromatid cohesion, and mitotic progression. Curr Biol. 16(9):863–874. doi:10.1016/j.cub.2006.03.049.

Woodman J, Hoffman M, Dzieciatkowska M, Hansen KC, Megee PC. 2015. Phosphorylation of the Scc2 cohesin deposition complex subunit regulates chromosome condensation through cohesin integrity. Mol Biol Cell. 26(21):3754–3767. doi:10.1091/mbc.E15-03-0165.

Wutz G, Ladurner R, St Hilaire BG, Stocsits RR, Nagasaka K, Pignard B, Sanborn A, Tang W, Várnai C, Ivanov MP, *et al.* 2020. ESCO1 and CTCF enable formation of long chromatin loops by protecting cohesin^{STAG1} from WAPL. Elife. 9:e52091. doi:10.7554/eLife.52091.

Xiang S, Koshland D. 2021. Cohesin architecture and clustering in vivo. Elife. 10:e62243. doi:10.7554/eLife.62243.

Yoshimura A, Sutani T, Shirahige K. 2021. Functional control of Eco1 through the MCM complex in sister chromatid cohesion. Gene. 784:145584. doi:10.1016/j.gene.2021.145584.

Zhang H, Blobel GA. 2023. Genome folding dynamics during the M-to-G1-phase transition. Curr Opin Genet Dev. 80:102036. doi:10.1016/j.gde.2023.102036.

Zhang N, Pati D. 2009. Handcuff for sisters: a new model for sister chromatid cohesion. Cell Cycle. 8(3):399–402. doi:10.4161/cc.8.3.7586.

Zhang J, Shi D, Li X, Ding L, Tang J, Liu C, Shirahige K, Cao Q, Lou H. 2017. Rtt101-Mms1-Mms22 coordinates replication-coupled sister chromatid cohesion and nucleosome assembly. EMBO Rep. 18(8):1294–1305. doi:10.15252/embr.201643807.

Zhang J, Shi X, Li Y, Kim BJ, Jia J, Huang Z, Yang T, Fu X, Jung SY, Wang Y, *et al.* 2008. Acetylation of Smc3 by Eco1 is required for S phase sister chromatid cohesion in both human and yeast. Mol Cell. 31(1):143–151. doi:10.1016/j.molcel.2008.06.006.

Zuilkoski CM, Skibbens RV. 2020. PCNA promotes context-specific sister chromatid cohesion establishment separate from that of chromatin condensation. Cell Cycle. 19(19):2436–2450. doi:10.1080/15384101.2020.1804221.

Zuilkoski CM, Skibbens RV. 2022. Integrating sister chromatid cohesion establishment to DNA replication. Genes (Basel). 13(4):625. doi:10.3390/genes13040625.

Editor: J. Surtees

Downloaded from https://academic.oup.com/genetics/advance-article/doi/10.1093/genetics/iyaf107/8159691 by guest on 23 June 2025